



저작자표시-비영리-변경금지 2.0 대한민국

이용자는 아래의 조건을 따르는 경우에 한하여 자유롭게

- 이 저작물을 복제, 배포, 전송, 전시, 공연 및 방송할 수 있습니다.

다음과 같은 조건을 따라야 합니다:



저작자표시. 귀하는 원저작자를 표시하여야 합니다.



비영리. 귀하는 이 저작물을 영리 목적으로 이용할 수 없습니다.



변경금지. 귀하는 이 저작물을 개작, 변형 또는 가공할 수 없습니다.

- 귀하는, 이 저작물의 재이용이나 배포의 경우, 이 저작물에 적용된 이용허락조건을 명확하게 나타내어야 합니다.
- 저작권자로부터 별도의 허가를 받으면 이러한 조건들은 적용되지 않습니다.

저작권법에 따른 이용자의 권리는 위의 내용에 의하여 영향을 받지 않습니다.

이것은 [이용허락규약\(Legal Code\)](#)을 이해하기 쉽게 요약한 것입니다.

[Disclaimer](#)

이학석사 학위논문

북부 동중국해 해수의 부유 물질 내 C₃₇
알케논

Long chain (C₃₇) alkenones in suspended materials
in the northern East China Sea



지도교수 이경은

2018년 2월


한국해양대학교 해양과학기술전문대학원

해양과학기술융합학과

고태욱

본 논문을 고태욱의 이학석사 학위논문으로 인준함.

위원장	이 희 준	(인)
위원	이 경 은	(인)
위원	장 태 수	(인)



2018년 1월

한국해양대학교 해양과학기술전문대학원

Contents

List of Figures	iv
List of Appendix	vi
Abstract	vii
1. Introduction	1
2. Materials and methods	
2.1 Study area	4
2.2 Sampling	6
2.3 Alkenone analysis	7
3. Results	
3.1 Surface seawater	9
3.2 Subsurface seawater	14
4. Discussion	
4.1 Alkenone unsaturation index as a temperature proxy	17
4.2 Alkenone concentration as a productivity proxy	21
5. Conclusions	25
Acknowledgement	26
References	27

List of Figures

- Fig. 1** (a) Study area with ocean currents in the East China Sea (KC: Kuroshio Current, TC: Taiwan Current, TWC: Tsushima Warm Current, EKWC: East Korea Warm Current, YSWC: Yellow Sea Warm Current, and CCC: Chinese Coastal Current). (b) Topographic map with station numbers. Red dot indicates station for subsurface seawater sampling 5
- Fig. 2** Monthly mean sea surface (a) temperatures and (b) salinities (WOA 2013, 1955-2012) 6
- Fig. 3** Concentration of total C₃₇ alkenones for surface seawater samples in the East China Sea (ng/L). ND means that samples were there but alkenones were not detected. Some surface seawater samples were collected during sailing. The line connecting dots indicates the sampling track. 11
- Fig. 4** Measured *in situ* SST for surfaces seawater samples in the northern East China Sea (°C). The line indicates the sampling track. 12
- Fig. 5** Alkenone temperatures for surface seawater in the northern East China Sea (°C). The line indicates the sampling track. 13
- Fig. 6** Vertical distribution of total C₃₇ alkenone at stations 315-12 and 317-13 (ng/L) 15
- Fig. 7** Vertical distribution of CTD-measured temperature and alkenone -based temperature at station 315-12 and 317-13. Solid line indicates CTD temperatures. Red square indicates alkenone temperatures. 16
- Fig. 8** Comparison of alkenone unsaturated index with *in situ* SST of surface water samples in the (a) eastern part of the study area and (c)

western part of the study area. Red line indicates the calibration equation of Prahl et al. (1988). Orange line represents the calibration equation of Conte et al. (2006). The difference between alkenone temperatures calculated by Prahl. (1988) and *in situ* SST in (b) the eastern part of the study area and (d) western part of the study area. 19

Fig. 9 Chlorophyll-*a* concentration in the surface seawater in February, May, August, and November during 2000–2005 (data from NFRDI of Korea, 2007). The dots indicate the locations of the stations used in this study.

..... 23



List of Appendix

Appendix 1. Data for surface samples during research cruise.	32
Appendix 2. Data for subsurface samples during research cruise.	36



Long chain (C₃₇) alkenones in suspended materials in the northern East China Sea

Ko, Tae Wook

Department of Convergence Study on the Ocean Science and
Technology

Korea Maritime and Ocean University
Ocean Science and Technology School

Abstract

The temporal and spatial distributions of long chain (C₃₇) alkenones in suspended materials in the northern East China Sea (ECS) were investigated to examine the applicability of using the degree of unsaturation of alkenones as a proxy for sea surface temperature (SST) and total C₃₇ alkenone concentration as a proxy for marine primary productivity. Sea water samples were collected at three-month intervals (February, May, August and November) during 2007-2010. The results showed that alkenones were synthesized throughout a year, with peaks in May. Alkenone temperatures corresponded to *in situ* temperatures. The vertical distribution of alkenone concentration showed that the alkenone production depth is the surface mixed layer (0-20 m). These results indicate that alkenone temperatures from marine sediments on the continental shelf most likely

reflect the annual average SST. No clear inferences could be made on the influence of nutrients and salinity on the alkenone temperature in this area. Seasonal changes in alkenone concentration were compared with those of chlorophyll-*a* concentration to investigate the suitability of using alkenone concentration as a productivity proxy. Where the chlorophyll-*a* concentration was high, the alkenone concentration was low, and vice versa, because the main primary producer was not coccolithophores. Therefore, it is not appropriate to use alkenone concentration as a primary productivity proxy in the ECS. However, comparisons to coccolithophore abundances show that it can be used as a haptophyte productivity proxy in this area.

KEY WORDS: Sea surface temperature; Paleothermometer; Productivity; Particulate organic matter; *Emiliana huxleyi*.



북부 동중국해 해수의 부유 물질 내 C₃₇ 알케논

고 태 욱

한국해양대학교 해양과학기술전문대학원

해양과학기술융합학과



초 록

동중국해 북부의 과거 표층 수온의 프록시로서 C₃₇ 알케논을 사용하는 것이 적합한지 확인하기 위하여 북부 동중국해 해수의 부유물질 내 C₃₇ 알케논 농도의 시간과 공간에 따른 변화를 조사하였다. 국립수산과학원에서 2007부터 2010년까지 실시한 동중국해 탐사에 참여하여 해수 시료를 채취하였다. 계절에 따른 알케논 농도 변화를 확인하기 위하여 매년 3개월 간격으로 채수하였다. 연구지역에서 알케논은 연중 합성되었으며 5월에 일시적으로 그 농도가 증가하였다. 표층 해수 시료의 알케논 복원 온도는 대체로 실측온도와 일치하였다. 알케논 농도의 수직분포를 보면 알케논이 주로 합성되는 수심은 표층부터 수심 20 m구간으로 이는 표층 혼합층에 해당한다. 이러한 결과들은 대륙붕지역에서 해양 퇴적물로부터 복원된 알케논 온도가 연평균 표층수온을 반영하는 것과 일치한다. 알케논 농도를 일차생산량의 프록시로서 사용하는 것이 적합한지 알아보기 위하여 클로로필-*a*의 계절에 따른 농도변화와 알케논 농도의 계절 변화를 비교하였다. 연구지역에서 클로로필-*a*의 농

도와 알케논 농도는 서로 반대되는 양상을 보였고 이는 이지역의 주요 일차 생산자가 석회비늘편모조류가 아니기 때문인 것으로 생각된다. 그러므로 동중국해 북부지역에서 일차생산성의 프록시로 알케논 농도를 사용하는 것은 적합하지 않은 것으로 보인다. 하지만 석회비늘편모조류의 개체 수와 비교하였을 때 알케논 농도는 착편모조류의 생산성 프록시로서 사용할 수 있을 것으로 생각된다.

주제어: 해수 표층 수온; 과거온도지시자; 생산성; 입자성유기물질; *Emiliana huxleyi*.

※ 이 석사학위논문에 게재된 대부분의 내용과 그림은 국제전문학술지인 *Palaeogeography, Palaeoclimatology, Palaeoecology*에 게재 확정되어 출판될 예정이다.



Chapter 1. Introduction

C₃₇ alkenones are long-chain unsaturated ketones synthesized by haptophyte microalgae living near the sea surface. The molecular biomarkers in marine sediments contain valuable information about sea surface temperature (SST) and, presumably, marine primary productivity in the past. The degree of unsaturation of C₃₇ alkenones (U_{37}^k) has been widely used as a proxy for past SST. Since Brassell et al. (1986) suggested that the degree of unsaturation of alkenones depends on the surrounding seawater temperature, the relationship has been calibrated based on culture experiments in the laboratory (Prahl et al., 1988) and comparisons between global core top U_{37}^k and annual mean SSTs (Müller et al., 1998). According to the studies, the relationship is generally linear. However, other factors, such as alkenone production depth and season, can influence the relationship (e.g., Herbert, 2001; Lee and Schneider, 2005; Harada et al., 2006; Popp et al., 2006). Since the maximum alkenone production depth and season can vary from one region to another, these factors must be taken into consideration before reconstructing past SSTs from alkenones of marine sediments. One of the best ways to explore the factors is to investigate spatial and temporal distribution patterns of C₃₇ alkenones by collecting seawater samples horizontally, vertically and seasonally at a study area (e.g., Lee et al., 2014).

C₃₇ alkenone abundance in sediments has been used in the past as a proxy for a specific type of algal productivity and total primary productivity (e.g., Rostek et al., 1997; Werne et al., 2000). Prahl and Muehlhausen (1989) showed that total alkenone concentrations per cell are essentially constant in living

cells. The properties of the alkenones preserved in sediments are quite similar to those observed in the sediment trap particles, which suggests that alkenones are considerably more resistant to biodegradation in the sedimentation process than most other lipids of planktonic origin (e.g., Prahl et al., 1988). Comparisons of alkenone concentration and other primary productivity proxies (e.g., $\delta^{13}\text{C}$ of total organic carbon) in sediments show that they are correlated for a given oceanic location (e.g., Jasper, 1988). However, since an algal source of these compounds is restricted to a narrow range of marine algae haptophyte, the downcore profiles of alkenone abundance in sediments would provide changes in haptophyte productivity, not changes in total primary productivity. Therefore, it is necessary to determine if alkenone concentration can provide a direct measure of biomass before this tool is applied.

The East China Sea (ECS) is in the northwestern Pacific margin and is connected to the Yellow Sea to the north, the South China Sea to the south and the subtropical North Pacific to the east. The shallow western part (< 100 m) is influenced by Yangtze River-diluted water with low temperature, low salinity, and high nutrients, whereas the relatively deep eastern part (> 100 m) is dominated by Kuroshio water with high temperature, high salinity, and low nutrients. The environmental characteristics will provide a good opportunity to test the effects of not only temperature but also nutrient and salinity on the U_{37}^k . Several studies investigated the distribution of C_{37} alkenones in areas adjacent to the ECS. Wu et al. (2016) investigated suspended particles of the Yellow Sea collected in spring and summer. Xing et al. (2011) and Tao et al. (2011) examined the distribution of lipid biomarkers from core tops of the Yellow Sea. According to Lee et al. (2014), alkenone-based temperatures from seawater samples at coastal stations of the East Sea corresponded well with summer-to-fall SSTs, whereas they agreed

better with annual mean SSTs at offshore stations. However, the distribution of C₃₇ alkenones in the ECS and the applicability of using alkenone as an SST proxy are not yet clear. Past SST reconstruction of this area is very important to understand changes in the Kuroshio and the East Asia monsoon system in the past. Moreover, since most studies on past SST reconstruction from alkenones have been conducted by using marine sediments from world-wide continental margins (e.g., world-wide data synthesis of the MARGO Project members, 2009), this kind of study will help to better understand the applicability of this technique.

In this study, we analyzed the seasonal and vertical distribution of alkenones in suspended materials in the northern ECS to investigate seasonality in alkenone production and variation in the depth of maximum alkenone production. Then, alkenone-based temperatures were compared with measured seawater temperatures to confirm if alkenone temperatures agreed with observed seawater temperatures. Finally, we explored the influence of factors other than seawater temperature on U_{37}^k such as nutrient and salinity. Additionally, alkenone concentrations were compared with chlorophyll-*a* concentrations in the northern ECS to test the reliability of using alkenone concentration as a proxy for primary productivity.

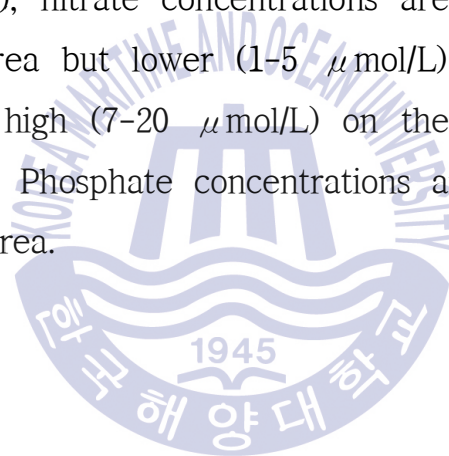
Chapter 2. Materials and methods

2.1 Study area

The ECS is surrounded by the northern Taiwan (25° N), the Jeju Island, Korea (33° N), mainland China and the Ryukyu and western Japanese islands. The shallow continental shelf (< 200 m) accounts for > 70% of this area. The Kuroshio Current flows northward along the continental slope (Fig. 1) and then divides at approximately 30° N (Lie and Cho, 2016). The major portion of the Kuroshio Current flows into the Pacific near the south of Kyushu, and the remaining flow is directed northwestward. This northwestward flow subdivides further into the Tsushima Warm Current and the Yellow Sea Warm Current, which flow toward the East Sea and the Yellow Sea, respectively. The Taiwan Warm Current passes the Taiwan Strait between the Chinese mainland and Taiwan Island and eventually runs into the ECS. The China Coastal Current moves southward along the Chinese coast in the Yellow Sea. Our study area is located on the continental shelf in the northern part of the ECS. Three transects are located over latitudes of 31.5–32.5° N, 124–127.5° E (Fig. 1). The water depth of the western part of the study area is approximately between 40 m and 100 m and that of the eastern part ranges between 100 m and 130 m.

The temperature across the northern ECS in summer varies little and remains between 26–28°C, based on the World Ocean Atlas 2013 (WOA 2013) from 1955 to 2012 (Fig. 2(a)). However, there is a noticeable temperature difference between the eastern and western parts of the ECS in winter; the

temperature of the eastern part is 15–18°C, whereas that of the western part is 10–15°C. The eastern part of the ECS has higher temperatures because of the Kuroshio Current. Diluted water from the Yangtze River flows into the western area of the ECS to the south of Jeju Island. This inflow varies seasonally. The discharge from the Yangtze River is greatest in summer and lowest in winter. Seasonal mean surface salinity is presented in Fig. 2(b). The salinity of the study area is 32–35 psu in winter and 30–33 psu in summer. According to seasonal and spatial variability of nutrients, such as nitrate, silicate and phosphate (the National Fisheries Research and Development Institute (NFRDI) serial oceanographic observation dataset, <http://kodc.nifs.go.kr/kodc>), nitrate concentrations are relatively high (4–15 μ mol/L) in the coastal area but lower (1–5 μ mol/L) in the offshore. Silicate concentrations are also high (7–20 μ mol/L) on the shelf and low (3–10 μ mol/L) in the outer sea. Phosphate concentrations are always less than 1 μ mol/L across the study area.



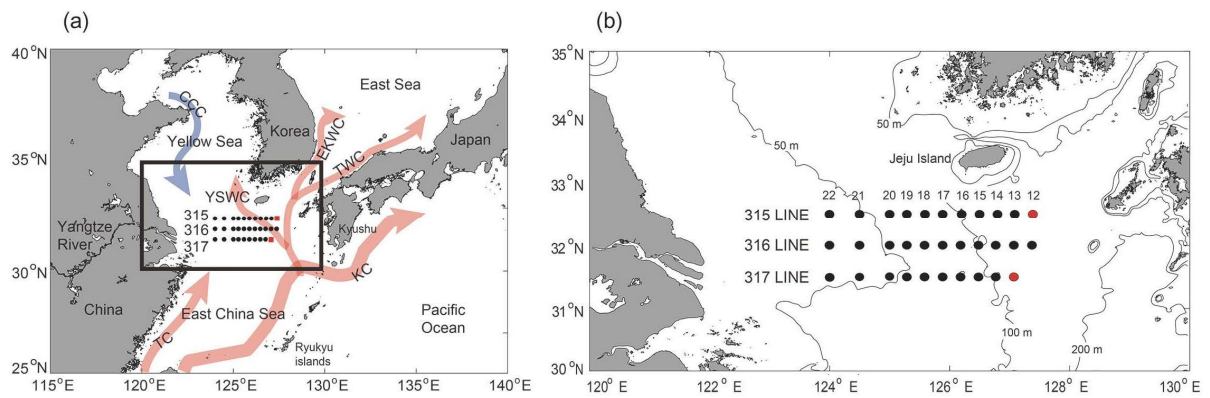


Fig. 1 (a) Study area with ocean currents in the East China Sea (KC: Kuroshio Current, TC: Taiwan Current, TWC: Tsushima Warm Current, EKWC: East Korea Warm Current, YSWC: Yellow Sea Warm Current, and CCC: Chinese Coastal Current). (b) Topographic map with station numbers. Red dot indicates station for subsurface seawater sampling.



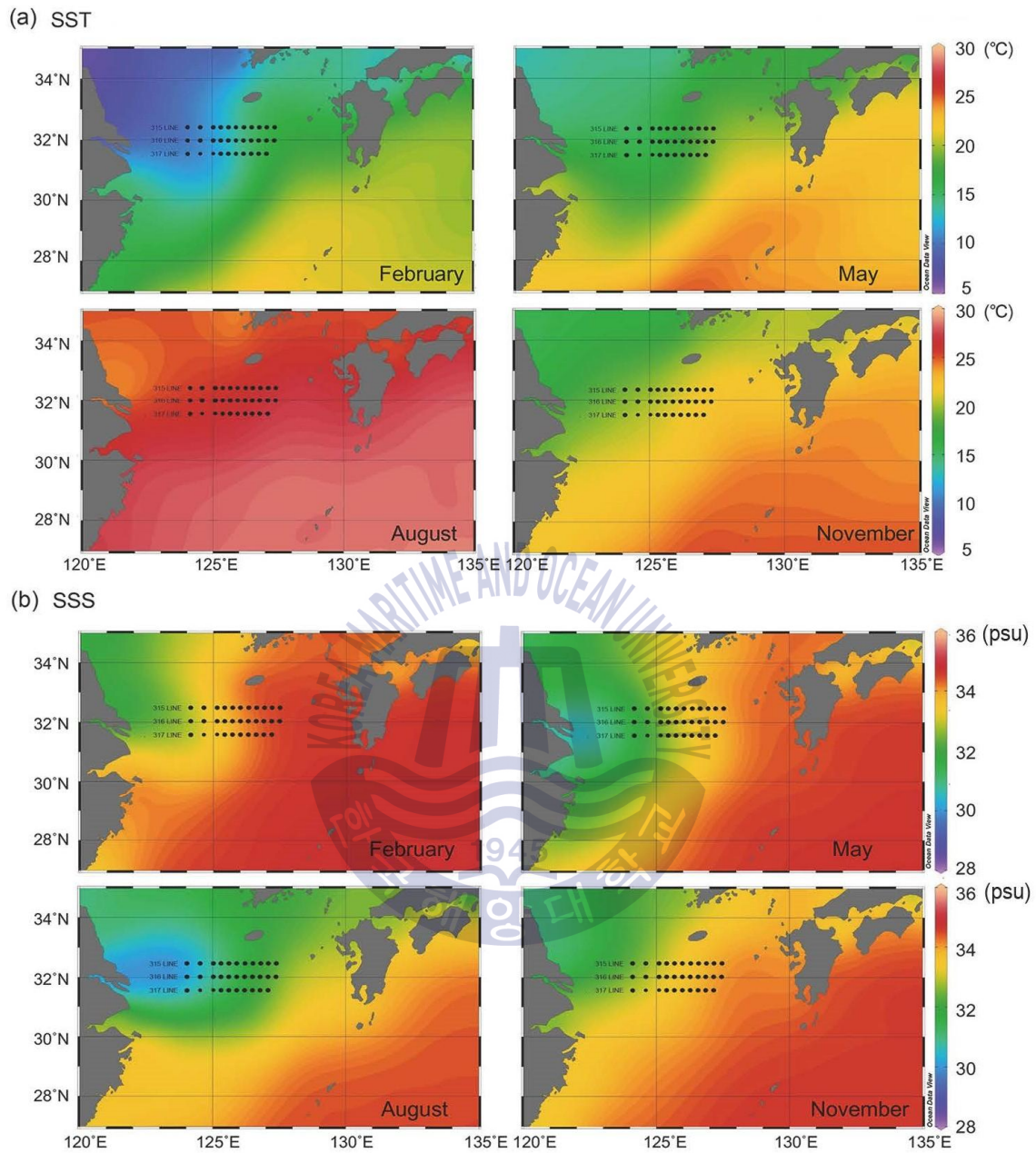


Fig. 2 Monthly mean sea surface (a) temperatures and (b) salinities (WOA 2013, 1955–2012).

2.2 Sampling

Seawater samples were collected at three-month intervals from February 2007 to August 2010 (Feb., May, Aug., and Nov.) along three transects during the NFRDI Korea research cruises (Fig. 1). Samples were divided into surface and subsurface seawater samples. Surface seawater samples were collected using a membrane pump at stations and during transit between stations. Samples of 100 L were collected and immediately filtered through glass fiber filters (GF/F, Whatman, 0.7 μ m) on ship. Subsurface samples were taken at water depths of 20 m and 50 m at two stations: station 315-12 (water depth, 128 m) and station 317-13 (water depth, 103 m). Exceptional samples were collected from station 315-22 (not from station 315-12) on November 2007 at depths of 20 m and 30 m. A rosette sampler with the CTD was used to collect subsurface seawater samples. Collected samples were immediately filtered by GF/F and stored below -25°C before alkenone analysis.

2.3 Alkenone analysis

Filter samples were freeze dried below -25°C in a freeze dryer (Yamato Science, DC400). Then, an internal standard (2-nonadecanone) was added to each sample. Samples were extracted using an accelerated solvent extractor (Dionex, ASE-200) at 100°C and 1,500 psi for 15 minutes with a mixture of solvents ($\text{CH}_2\text{Cl}_2:\text{CH}_3\text{OH}, 99:1\text{v/v}$). Extracts completely dried under N_2 and concentrated were saponified with 0.1M KOH in CH_3OH at 70°C for 2 hours. Neutral lipids in the samples were then separated by hexane. Samples were then divided into four fractions (fr.) by using an automatic solid phase extraction system (Rapid Trace SPE workstation, Zymark). The composition of the solvent was as follows: 4mL of hexane (fr.1); a mixture of 2mL of hexane/toluene (3:1v/v), 2mL of hexane/toluene (1:1v/v), and 2mL of

hexane/ethyl acetate (19:1v/v) (fr.2); a mixture of 2mL of hexane/ethyl acetate (18:2v/v) and 2mL of hexane/ethyl acetate (17:3v/v) (fr.3); and a mixture of 4mL of hexane/ethyl acetate (4:1v/v) and 2mL of ethyl acetate (fr.4). Fraction 3 contained alkenones and was dried entirely under N₂. These alkenones were quantified using a Flame Ionization Detector and fused-silica capillary column (J&W DB-1, 60m*0.32 mm*0.25 μm, Agilent Technology) attached to a Gas Chromatograph (Agilent 7890A). The alkenone unsaturation index was calculated from the equation (1) suggested by Prahl and Wakeham (1987):

$$U_{37}^{k'} = \frac{[C_{37:2}]}{[C_{37:2}] + [C_{37:3}]} \quad (1)$$

Alkenone temperatures were computed by using the equation (2) established by Prahl et al. (1988):

$$T = (U_{37}^{k'} - 0.039)/0.034 \quad (2)$$



Chapter 3. Results

3.1 Surface seawater

Variations in total C_{37} ($C_{37:3+}$ $C_{37:2}$) alkenone concentration in surface seawater samples are presented in Fig. 3. Alkenone concentrations were lowest in winter. There were many samples in which alkenones could not be detected in winter. Alkenone concentrations increased (by > 1 ng/L) in the eastern part of the study area in spring. In summer, the concentration patterns were different. Alkenones were not detected in August 2007 except on point (317-13). However, they increased higher than spring concentrations in August 2010. The concentrations ranged mostly between 0.1 and 0.5 ng/L in fall. When the concentrations in samples from the eastern stations (e.g., 315-12, 316-12, 317-13/14) were compared with those of the western stations (e.g., 315-22, 316-21/22, 317-22), the concentrations at eastern stations were always higher than those of the western area.

The *in situ* SSTs recorded by the CTD are presented in Fig. 4. The *in situ* SSTs in the study area were 8-17°C in February, 15-20°C in May, 27-29°C in August, and 18-23°C in November. SSTs in the western part of the study area were low and those of the eastern part were high. These results agree with monthly mean SST data of the WOA 2013 from 1955 to 2012. Reconstructed alkenone temperatures were as follows: 14-16°C in winter, 12-20°C in spring, > 28 °C in summer, and 15-23°C in fall (Fig. 5). Therefore, reconstructed alkenone temperatures are seasonal, similar to *in situ* temperatures. Alkenone temperatures for some of the samples collected in summer were above 28.

3°C. Because C_{37:3} was not detected and only C_{37:2} was detected, $U_{37}^{k'}$ was 1 in these samples. The differences between alkenone temperatures and *in situ* temperatures were approximately within $\pm 2^\circ\text{C}$.



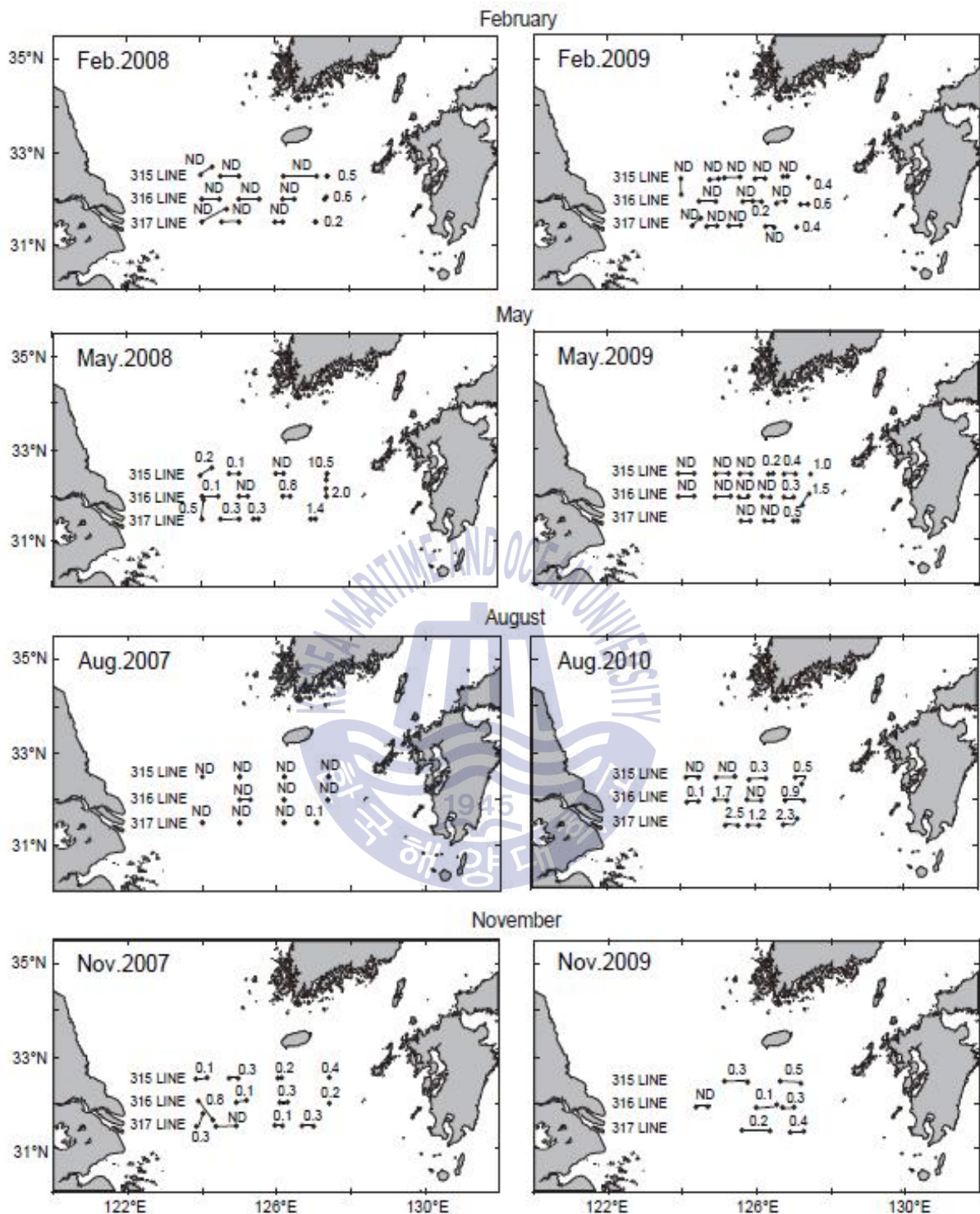


Fig. 3 Concentration of total C₃₇ alkenones for surface seawater samples in the East China Sea (ng/L). ND means that samples were there but alkenones were not detected. Some surface seawater samples were collected during sailing. The line connecting dots indicates the sampling track.

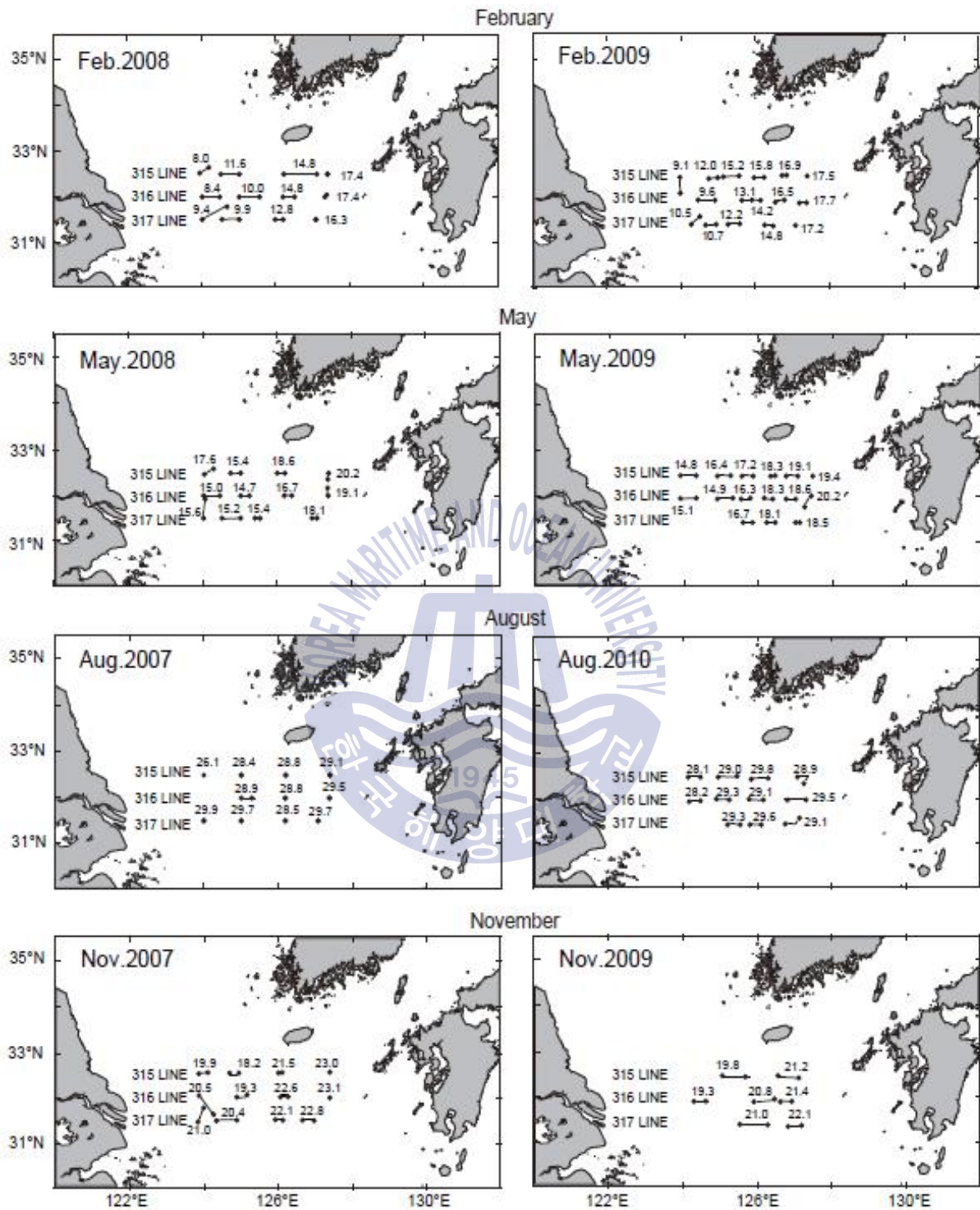


Fig. 4 Measured *in situ* SST for surfaces seawater samples in the northern East China Sea (°C). The line indicates the sampling track.

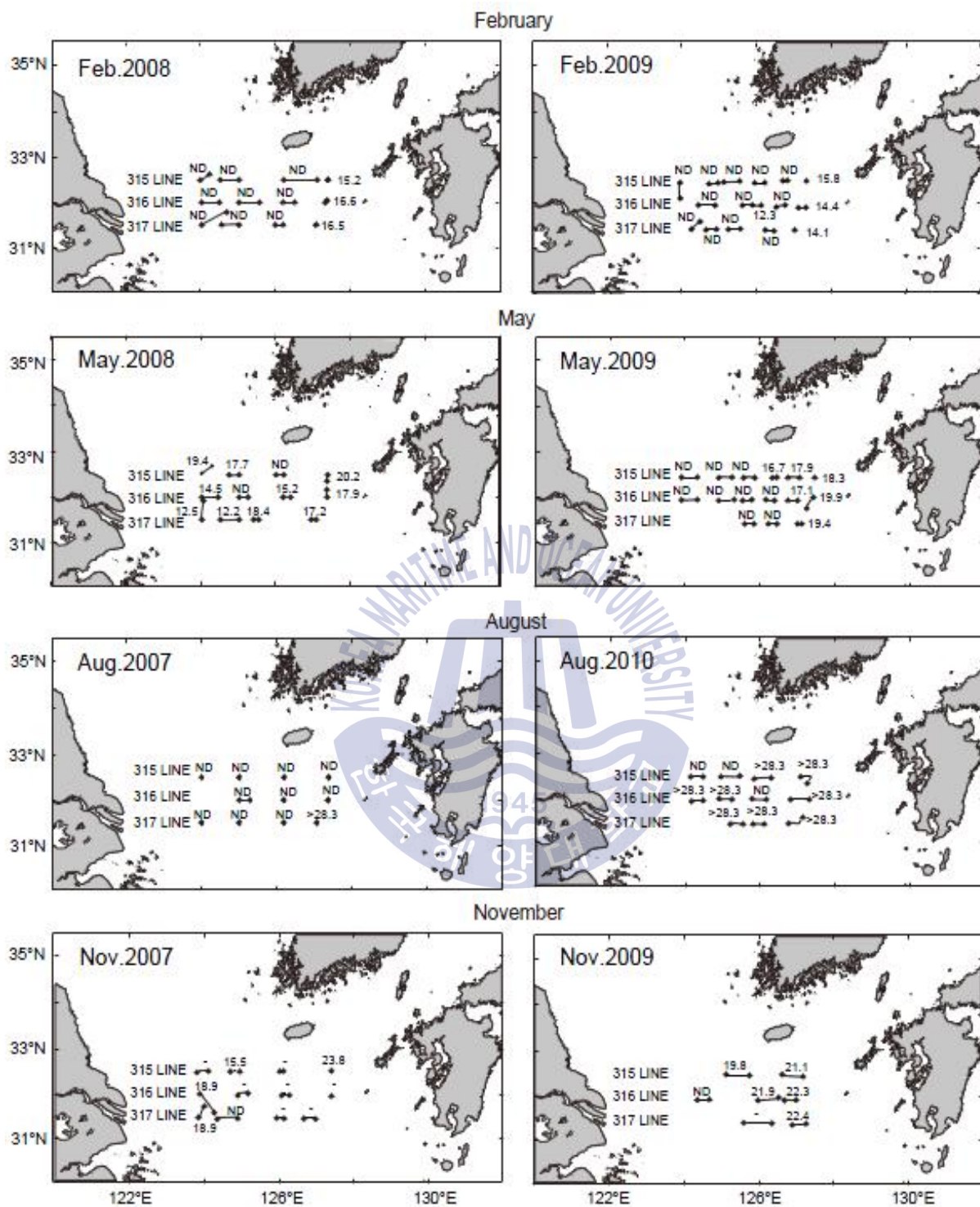


Fig. 5 Alkenone temperatures for surface seawater in the northern East China Sea (°C). The line indicates the sampling track.

3.2 Subsurface seawater

Total C₃₇ alkenone concentrations from subsurface sea water samples of stations 315-12 (32.5° N, 127.5° E) and 317-13 (31.5° N, 127° E) are shown in Fig. 6. The concentrations in most seasons increased at 20 m but considerably decreased at 50 m. Therefore, the vertical distribution of the concentrations shows that the concentrations were highest near the surface (0-20 m). The alkenone concentrations of subsurface water samples were relatively high in May 2008, May 2009, and August 2010, which supports the seasonality of alkenone concentrations from surface seawater samples. Depth profiles of alkenone temperatures and *in situ* temperatures are illustrated in Fig. 7. *In situ* temperatures were uniformly distributed in spring, fall, and winter. However, the temperatures in summer were both 29°C at the surface, and they significantly decreased below 10-30 m. Therefore, the surface mixed layer in summer extended from the surface to approximately 20 m, and a seasonal thermocline existed below the surface mixed layer. Alkenone temperatures were 14-17°C from the surface down to 50 m in winter, 19°C at the surface and 14-16°C below a depth of 20 m in spring. The temperatures were 23-26°C from the surface to a depth of 50 m in fall. In summer, alkenone temperatures were approximately 25°C at a depth of 20 m. Therefore, alkenone temperatures estimated from subsurface seawater samples generally seemed to correspond well with *in situ* temperatures, and the difference between them was generally within $\pm 2^\circ\text{C}$ at each depth surveyed.

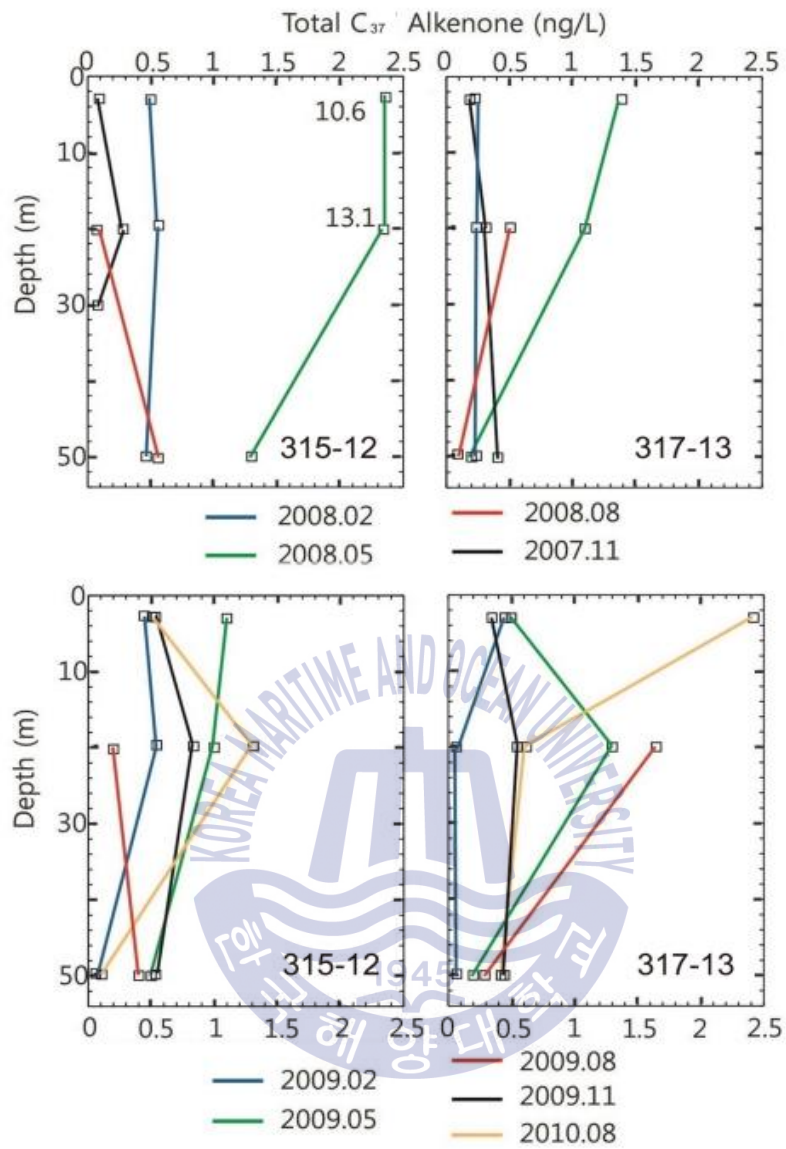
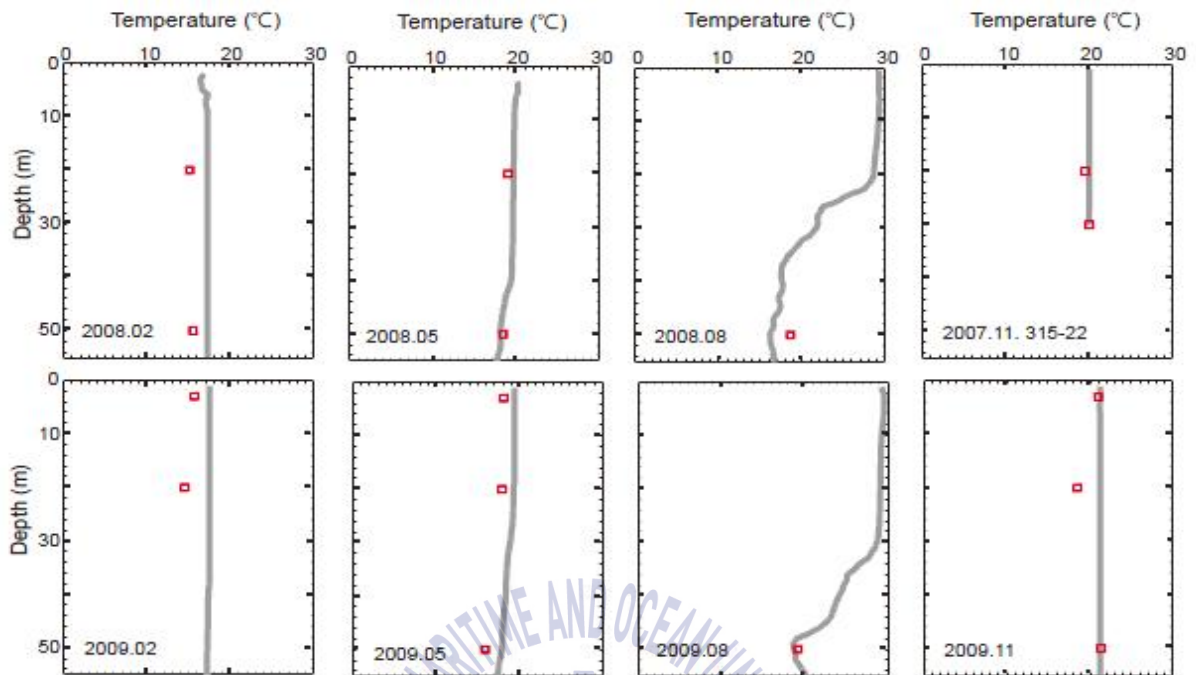


Fig. 6 Vertical distribution of total C₃₇ alkenone at stations 315-12 and 317-13 (ng/L)

ECS 315-12



ECS 317-13

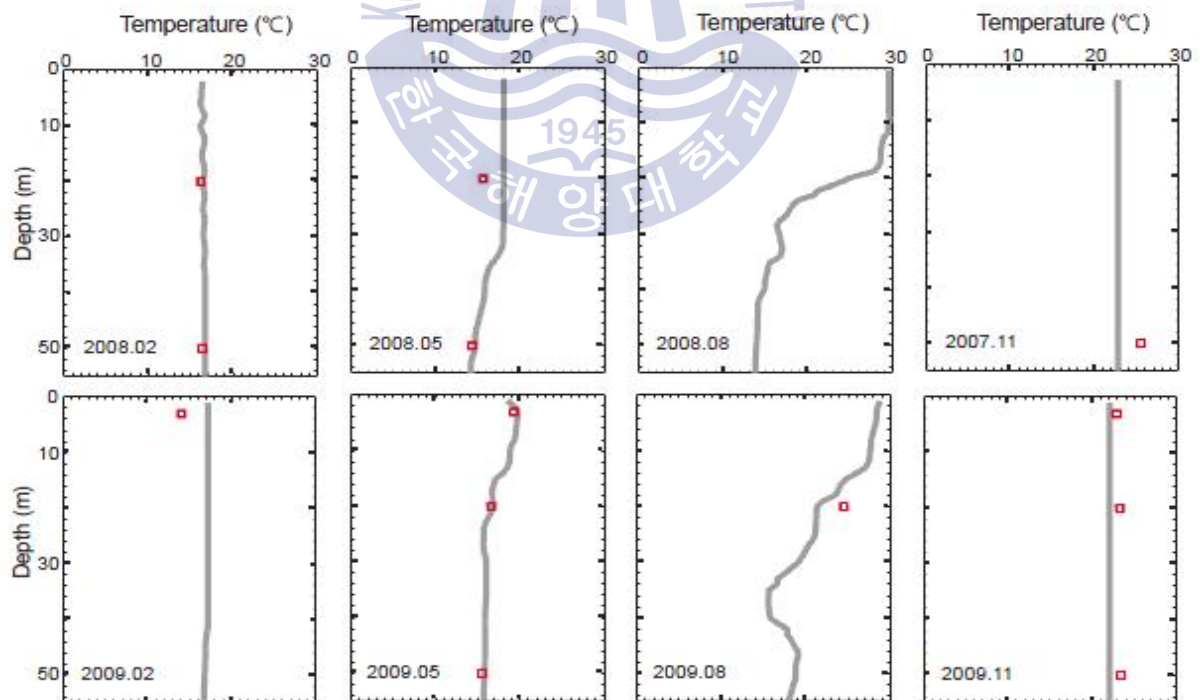


Fig. 7 Vertical distribution of CTD-measured temperature and alkenone-based temperature at station 315-12 and 317-13. Solid line indicates CTD temperatures. Red square indicates alkenone temperatures.

Chapter 4. Discussion

4.1 Alkenone unsaturation index as a temperature proxy

Alkenone temperatures reconstructed from sediments were generally assumed to reflect SST; maximum alkenone production should thus occur at the surface or within the surface mixed layer. Based on the vertical profile of alkenone concentration in this study, alkenones appear to have been synthesized in the surface mixed layer with a maximum at 20 m in the eastern area of the northern ECS. Alkenone temperatures estimated from suspended particles also corresponded well with *in situ* temperatures. These results indicate that alkenone temperatures reconstructed from the sediment of the northern ECS reflect SST.

Alkenone temperatures calculated from marine sediments samples have been presumed to reflect annual mean SST. This assumes that alkenone producers synthesize alkenones year-round. However, if alkenone production is specific to a particular season, alkenone temperatures from marine sediments would reflect seawater temperatures during that production season. Our results for the seasonal fluctuation of surface alkenone concentration in the eastern part of the northern ECS show that alkenones were synthesized throughout a year, with peaks in May, which indicates that alkenone temperatures from marine sediments in this area most likely reflect annual average SST. In contrast, alkenone concentration in the western part was very much lower than that of the eastern part year-round. It is probably due to low abundance of alkenone producers in the western part (see Section 4.2.). Reconstructed alkenone

temperatures from marine sediment core-top samples collected near transect 317 in the western part were 21.5°C at 31.3° N, 125.45° E (Zhao et al., 2014), 21.1°C at 31.73° N, 126.12° E (Xing et al., 2013), and 19.2°C at 31.68° N, 125.81° E (Li et al., 2009). Despite low alkenone concentration in the western area, the core-top alkenone temperatures were close to the annual average SST.

The relationships between measured U_{37}^k values (and alkenone temperatures) with *in situ* SSTs were displayed in Fig. 8 (a) and © with the calibration equations of Prahl et al. (1988) and Conte et al. (2006). Fig. 8 (b) and (d) presents the difference between alkenone temperatures calculated by the former equation and the *in situ* temperatures. In general, alkenone temperatures calculated by the Prahl et al. (1988) calibration equation did not significantly deviate from *in situ* temperatures. In the eastern part of the study area, most alkenone temperatures correlated with *in situ* temperatures within 2°C. The temperature differences in the western area were larger than 2°C. Several factors such as calibration equation, different alkenone producers, and physiology that could influence on the difference between alkenone temperature and *in situ* temperatures were considered in the followings.

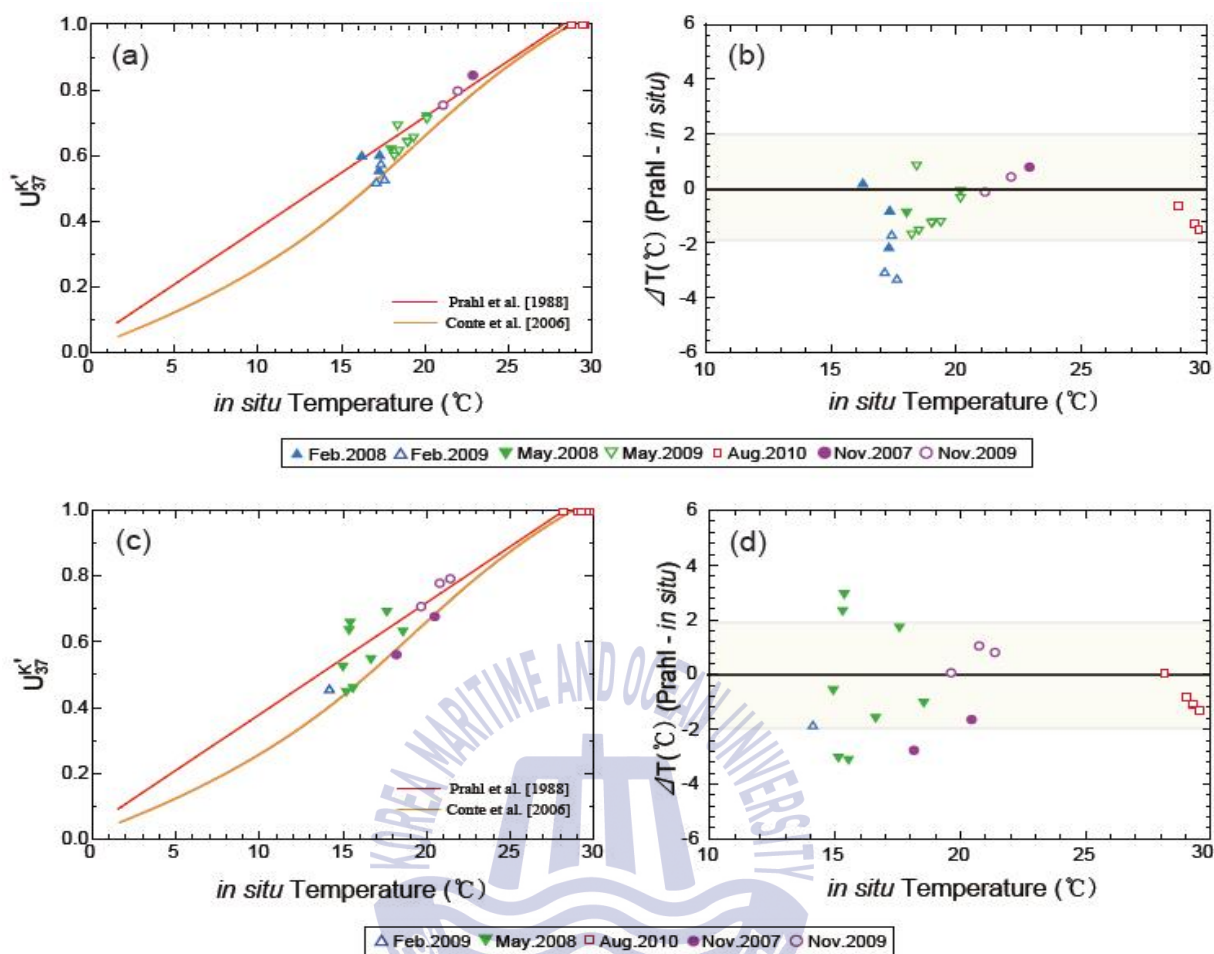


Fig. 8 Comparison of alkenone unsaturated index with *in situ* SST of surface water samples in the (a) eastern part of the study area and (c) western part of the study area. Red line indicates the calibration equation of Prahl et al. (1988). Orange line represents the calibration equation of Conte et al. (2006). The difference between alkenone temperatures calculated by Prahl. (1988) and *in situ* SST in (b) the eastern part of the study area and (d) western part of the study area.

The calibration equation of Prah1 et al. (1988) was constructed by using laboratory cultures of *Emiliania huxleyi*. However, alkenones are produced not only by *E. huxleyi* but also by *Gephyrocapsa oceanica*. Therefore, the calibration equation may need to be adjusted based on the major alkenone producers (Volkman et al., 1995). Tanaka (2003) presented a distribution of coccolithophores of the ECS coretop sediments, and confirmed that *E. huxleyi* is dominant closer to the Okinawa Trough, whereas *G. oceanica* is dominant closer to the Yangtze River estuary on the continental shelf. Recently, Luan et al. (2016) investigated the distribution of coccolithophores in the water column of the northern ECS in fall. *G. oceanica* increased to the south of 30° N, closer to the inner shelf, but *E. huxleyi* was dominant to the north of 30° N. Our study area is located between 31.5° N and 32.5° N, and *E. huxleyi* is thus relatively dominant in both eastern and western parts of the study area. The use of the calibration equation of Prah1 et al. (1988) is suitable because *E. huxleyi* is the main alkenone producer in this area. Moreover, when the Volkman et al. (1995) equation was applied to samples from all the stations, alkenone temperatures were between 20°C and 24°C, which is much higher than *in situ* temperatures and Prah1's equation results. Therefore, *G. oceanica* may not be a significant factor.

According to previous studies, some physiological factors influence U_{37}^k . Previous researchers have suggested that not only seawater temperatures but also nutrient concentration influences the degree of alkenone unsaturation. Popp et al. (1998) showed that variations of nutrients would not affect U_{37}^k ; however, Epstein et al. (1998) suggested that U_{37}^k also increased when concentrations of NO_x decreased, such that alkenone temperatures increased. Later, Prah1 et al. (2003) showed that if nitrates were reduced, U_{37}^k would decrease. Therefore, it is uncertain that U_{37}^k could increase or decrease

because of nutrient decrease. Influences of nutrients on U_{37}^k in this study area were investigated by an examination of the NFRDI nutrient dataset. Scatter plots of the linear regression analysis between nutrients and U_{37}^k showed that there was no significant relationship between them in the northern ECS at a 95% confidence level. The values of R^2 between nutrients and U_{37}^k were 0.065 for silicate, 0.041 for nitrate, and 0.002 for phosphate, which supports no relationship between them in the study area.

Another factor that influences the degree of alkenone unsaturation other than temperature may be salinity. Rosell-melé (1998) suggested that a higher relative abundance of $C_{37:4}$ ($\%C_{37:4} = ([C_{37:4}]/[C_{37:2}]+[C_{37:3}]+[C_{37:4}]))$ corresponded to fresher conditions in the salinity range of 33.5–35.5 at high latitude locations. The salinity distribution of the northern ECS is 28–30 in the western part in summer and 31–32 in the eastern part; in winter, it is 32–33 in the west and 33–34 in the east (NFRDI dataset). The occurrence of $C_{37:4}$ was examined to check the salinity influence on the degree of alkenone unsaturation. $C_{37:4}$ was not detected in any of the samples from the study area. Moreover, a scatter plot of the linear regression analysis between salinity and U_{37}^k showed that there was no significant relationship between them at a 95% confidence level; R^2 values were less than 0.1. Therefore, it is unlikely that salinity affects the degree of the unsaturation in the northern ECS.

4.2 Alkenone concentration as a productivity proxy

Seasonal changes in total C_{37} alkenone concentrations were compared with those of chlorophyll-*a* concentration (NFRDI dataset, 2007) to confirm the suitability of using alkenone concentration as a proxy for primary productivity in the study area. Fig. 9 presents the seasonal distribution of chlorophyll-*ain*

the study area. The chlorophyll-*a* values were generally 0.4-0.6 $\mu\text{g/L}$ throughout the study area in winter. In spring, chlorophyll-*a* ranged from ~ 0.8 to 1 $\mu\text{g/L}$ in the western part of the study area and from ~ 0 to 0.4 $\mu\text{g/L}$ in the east. In summer, the concentrations ranged from ~ 0.6 to 1 $\mu\text{g/L}$ in the western part and from ~ 0 to 0.4 $\mu\text{g/L}$ in the east. In fall, concentrations were generally 0.3-0.5 $\mu\text{g/L}$ throughout the study area. Therefore, the concentrations of chlorophyll-*a* concentrations from the western part were generally higher than those of the eastern area. A strong winter monsoon caused strong vertical mixing such that nutrients rose from the bottom to the surface water layer, which resulted in high chlorophyll-*a* (and productivity) in winter. In spring and summer, the presence of the diluted Yangtze River plume in the study area increased stratification (and enhanced solar insolation) in the upper layers. This stratification disturbed the supply of nutrients from the bottom to the surface. However, this could be offset by the nutrients supplied by the Yangtze River plume such that the chlorophyll-*a* concentrations indicated fairly high productivity in the western part of the study area in spring and summer. In contrast to the distribution of chlorophyll-*a*, alkenones were hardly detected anywhere within the study area in winter. Additionally, alkenone concentrations were high in the eastern part of the study area in spring, although the concentrations in the west were very low in spring. Alkenone concentrations were low where the contents of chlorophyll-*a* were high, and vice versa, likely because the main chlorophyll-*a* producers were not coccolithophores. Previous studies of phytoplankton population distributions in the northern ECS have suggested that diatoms dominate along the coast near the Yangtze River estuary and dinoflagellates dominate near the front (Yoon et al., 2003). Therefore, using alkenone concentration as a proxy of primary productivity is not applicable in this area.

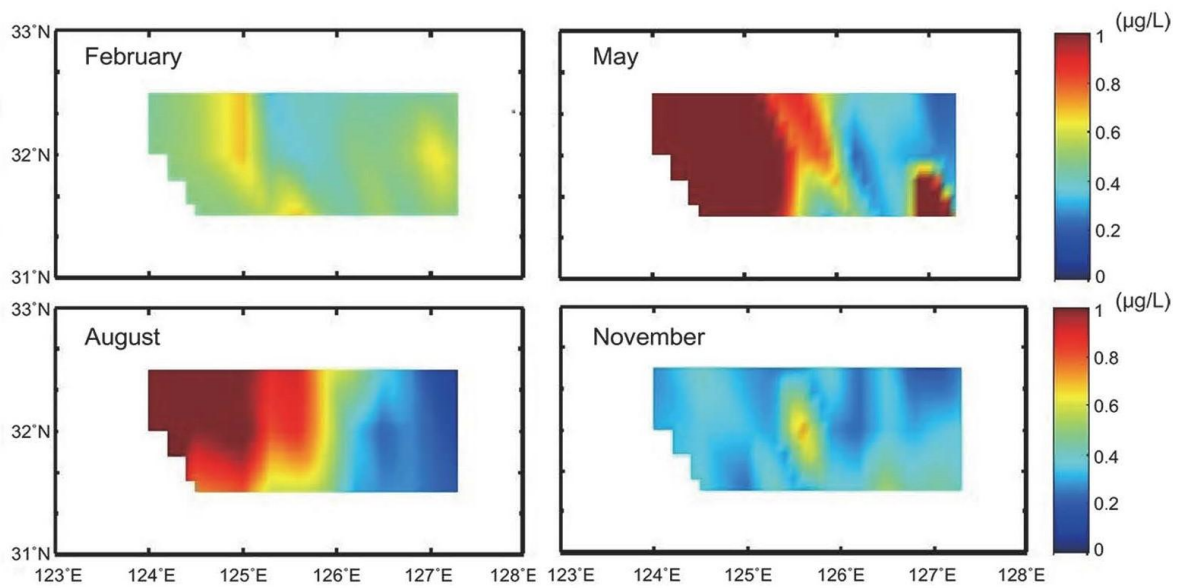
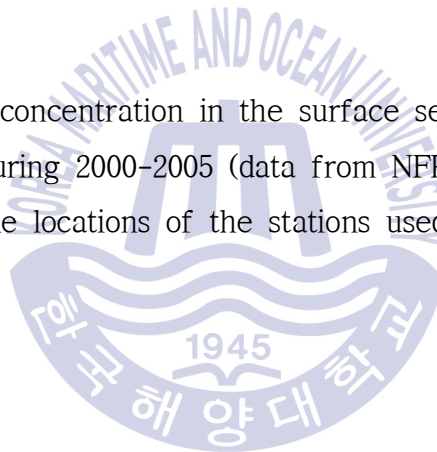


Fig. 9 Chlorophyll-a concentration in the surface seawater in February, May, August, and November during 2000–2005 (data from NFRDI of Korea, 2007). The dots indicate the locations of the stations used in this study.



The distribution of total C₃₇ alkenone concentration was compared with those of living coccolithophore abundance in the water column of the ECS. According to Sun et al. (2014), *E. huxleyi* abundance was low (0–2 cells/mL) in the western part and relatively higher (> 5 cells/mL) in the eastern part in winter (Dec.20, 2011–Jan.12, 2012), while the abundance was 0–2 cells/mL in summer (July 6–24, 2011). *G. Oceanica* abundance was higher than 5 cells/mL at both western and eastern parts in winter, but it was 0–3 cells/mL in summer (Sun et al.,2014). Luan et al. (2016) showed distribution of living coccolithophores in fall (Oct.13–Nov.16, 2013) in the ECS. *E. huxleyi* abundance was 10 and 17 cells/mL in the western and eastern part in fall, respectively. *G. oceanica* abundance was 0 cells/mL in the west and 3 cells/mL in the east. Hence, simple calculations show that the total abundance of two species seem to be approximately 5–10 cells/mL in winter, 0–5 cells/mL in summer and 10–20 cells/mL in fall. Although there was no spring record of living coccolithophores abundance in both datasets, the alkenone producers appear to inhabit in the study area throughout a year. Our records show low alkenone concentration in both winter and summer, although summer concentration patterns were different in 2007 and 2010. Notably, the abundance of living coccolithophores was low in the western part and increased in the eastern part in fall and winter, which was similar to total C₃₇ alkenone concentration pattern. This suggests that the total C₃₇ alkenone concentration can be used as a Haptophyte productivity proxy in the area.

Chapter 5. Conclusions

In the northern ECS, alkenones were produced in the surface mixed layer with a maximum between the surface and 20 m. Therefore, alkenone temperatures from marine sediment samples in this area would reflect SSTs. Alkenones were synthesized throughout a year with peaks in May, which indicated that alkenone temperatures from marine sediments in this area likely to be close to annual average SST. There were no clear influences of nutrients and salinity on the degree of alkenone unsaturation. Alkenone concentrations were not positively correlated with chlorophyll-*a* concentrations. Alkenone concentrations were low when chlorophyll-*a* concentrations were high, and vice versa. Therefore, the potential use of alkenone concentration as a proxy for primary productivity in the ECS is limited. However, it can be used as a haptophyte productivity proxy in the area.

Acknowledgments

멀고도 험난한 과정이었습니다. 그만큼 소중한 결과물로 다가온 논문이 되었습니다. 3년간의 석사과정기간 중 가장 배우는 게 많았던 기간이 논문을 작성하던 이 시기가 아니었던가 라는 생각이 듭니다. 고생 끝에 얻은 데이터 하나 하나의 소중함을 일깨워 주시고, 명료하고 객관적이고 과학적으로 사고하고 그것을 글로 표현할 수 있도록 늘 지도해주시는 이경은 교수님께 진심으로 감사드립니다. 논문 쓰는 동안뿐만 아니라 다른 방면에서도 부족한 게 많은 저를 지도해 주시고 조언해 주시고 기회를 주신 덕분에 학부생 때와는 다르게 성장하고 발전할 수 있었다고 생각합니다.

바쁘신 와중에도 항상 제게 관심을 가져 주시고 이번 논문 또한 심사해주신 이희준 박사님과 장태수 교수님께 감사드립니다. 학교에 올 때마다 편안하게 조언해 주시는 지영이 누나, 본 논문의 데이터 정리를 도와주신 용기 형과 성혜 누나, 항상 옆자리에서 묵묵히 도와주는 시웅이 형, 연구실 생활 초기에 고민도 함께 들어주며 연구실 생활을 하는데 적응할 수 있게 도와준 령아, 나연이, 가희 모두에게 늘 감사한 마음을 갖고 있고 이 지면을 통해 말씀드립니다.

그리고 멀리 떨어져서 생활하는 아들이 잘하고 있는지 늘 걱정하시지만 항상 믿어주시고 지원해주시는 부모님께 감사드립니다.

References

- Brassell, S.C., Eglinton, G., Marlowe, I.T., Pflaumann, U., Sarnthein, M., 1986. Molecular stratigraphy: a new tool for climatic assessment. *Nature* 320, 129-133.
- Conte, M.H., Sicre, M.A., Ruhlemann, C., Weber, J.C., Schulte, S., Schulz-Bull, D., Blanz, T., 2006. Global temperature calibration of the alkenone unsaturation index in surface waters and comparison with surface sediments. *Geochemistry Geophysics Geosystem* 7, Q02005. doi:10.1029/2005GC001054.
- Epstein, B.L., D' Hondt, S., Quinn, J.G., Zhang, J., Hargraves, P.E., 1998. An effect of dissolved nutrient concentrations on alkenone-based temperature estimates. *Paleoceanography* 13, 122-126.
- Harada, N., Ahagon, N., Sakamoto, T., Uchida, M., Ikehara, M., Shibata, Y., 2006. Rapid fluctuation of alkenone temperature in the southwestern Okhotsk Sea during the Past 120 kyr. *Global Planetary Change* 53, 29-46.
- Herbert, T.D., 2001. Review of alkenone calibrations (culture, water column, and sediments). *Geochemistry Geophysics Geosystem* 2, 1055. doi:10.1029/2000GC000055.
- Jasper, J., 1988. An organic geochemical approach to problems of glacial-interglacial climatic variability. Ph.D. diss. Woods Hole Oceanographic Institution, p. 312. Retrieved from <https://hdl.handle.net/1912/4626>.
- Lee, K.E., and Schneider, R., 2005. Alkenone production in the upper 200 m of the Pacific Ocean. *Deep-Sea Research I* 52, 443-456.
- Lee, K.E., Lee, S., Park, Y., Lee, H.J., Harada, N., 2014. Alkenone production

- in the East Sea/Japan Sea. *Continental Shelf Research* 74, 1-10.
- Li, G., Sun, X., Liu, Y., Bickert, T., Ma, Y. 2009. Sea surface temperature record from the north of the East China Sea since late Holocene. *Chinese Science Bulletin* 54 (23), 4507-4513.
- Lie, H.J., Cho, C.H., 2016. Seasonal circulation patterns of the Yellow and East China Seas derived from satellite-tracked drifter trajectories and hydrographic observations. *Progress in Oceanography* 146 (2016), 121-141.
- Luan, Q., Liu, S., Zhou, F., Wang, J., 2016. Living coccolithophore assemblages in the Yellow and East China Seas in response to physical processes during fall 2013, *Marine Micropaleontology* 123, 29-40.
- MARGO Project Members (2009) Constraints on the magnitude and patterns of ocean cooling at the Last Glacial Maximum. *Nature Geoscience* 2 (2), 127-132. – Supplementary material. PANGAEA. doi: 10.1594/PANGAEA.733406.
- Müller, P.J., Kirst, G., Ruhland, G., Storch, I., Rosell-Melé, A., 1998. Calibration of the alkenone paleotemperature index U_{37}^k based on core tops from the eastern South Atlantic and the global ocean (60° N-60° S). *Geochimica Cosmochimica Acta* 62, 1757-1772.
- National Fisheries Research and Development Institute (NFRDI) (2007) *Data of chlorophyll-a and total suspended matter in the East China Sea: 2000-2005*.
- National Fisheries Research and Development Institute (NFRDI) serial oceanographic observation dataset. Retrieved from <http://kodc.nifs.go.kr/kodc>.
- Popp, B.N., Kening, F., Wakeham, S.G., Laws, E.A., Bidigare, R.R., 1998. Does growth rate affect keton unsaturation and intracellular carbon isotopic variability in *Emiliana huxleyi*? *Paleoceanography* 13, 35-41.
- Popp, B.N., Prahl, F.G., Wallsgrave, R.J., Tanimoto, J., 2006. Seasonal patterns of alkenone production in the subtropical oligotrophic North Pacific.

- Paleoceanography* 21, PA1004. doi: 10.1029/2005PA001165.
- Prahl, F.G., Wakeham, S.G., 1987. Calibration of unsaturation patterns in long-chain ketone compositions for palaeotemperature assessment. *Nature* 330, 367-369.
- Prahl, F.G., Muehlhausen, L.A., Zahnle, D.L., 1988. Further evaluation of long-chain alkenones as indicators of paleoceanographic conditions. *Geochimica Cosmochimica Acta* 52, 2303-2310.
- Prahl, F.G., Muehlhausen, L.A., 1989. *Lipid biomarkers as geochemical tools for paleoceanographic study. Productivity of the ocean: present and past*, 271-289.
- Prahl, F.G., Wolfe, G.V., Sparrow, M.A., 2003. Physiological impacts on alkenone paleothermometry. *Paleoceanography* 18 (2), 1025. doi:10.1029/2002PA000803.
- Rosell-Melé, A., 1998. Interhemispheric appraisal of the value of alkenone indices as temperature and salinity proxies in high-latitude locations, *Paleoceanography* 13 (6), 694-703. doi:10.1029/98PA02355.
- Rostek, F., Bard, E., Beaufort, L., Sonzogni, C., Ganssen, G., 1997. Sea surface temperature and productivity records for the past 240 kyr in the Arabian Sea. *Deep Sea Research Part II: Topical Studies in Oceanography* 44 (6-7), 1461-1480. doi:10.1016/S0967-0645 (97)00008-8.
- Sun, J., Gu, X.Y., Feng, Y.Y., Jin, S.F., Jiang, W.S., Jin, H.Y., Chen, J.F., 2014. Summer and winter living coccolithophores in the Yellow Sea and the East China Sea. *Biogeosciences* 11, 779-806. doi: 10.5194/bg-11-779-2014.
- Tanaka, Y., 2003. Coccolith fluxes and species assemblages at the shelf edge and in the Okinawa Trough of the East China Sea. *Deep-Sea Research Part II* 50, 503-511.

- Tao, S., Xing, L., Luo, X., Wei, H., Liu, Y., Zhao, M., 2011. Alkenone distribution in surface sediments of the southern Yellow Sea and implications for the U_{37}^k thermometer. *Geo-Marine Letters* 32 (1), 61–71.
- Volkman, J.K., Barrett, S.M., Blackburn, S.I., Sikes, E.L., 1995. Alkenones in *Gephyrocapsa oceanica*: implications for studies of paleoclimate. *Geochimica Cosmochimica Acta* 59, 513–520.
- Werne, J.P., Hollander, D.J., Lyons, T.W., Peterson, L.C., 2000. Climate-induced variations in productivity and planktonic ecosystem structure from the Younger Dryas to Holocene in the Cariaco Basin, Venezuela. *Paleoceanography* 15 (1), 19–29.
- Wu, P., Bi, R., Duan, S., Jin, H., Chen, J., Hao, Q., Cai, Y., Mao, X., Zhao, M., 2016. Spatiotemporal variations of phytoplankton in the East China Sea and the Yellow Sea revealed by lipid biomarkers. *Journal of Geophysical Research-Biogeosciences* 121, 109–125, doi:10.1002/2015JG003167,
- Xing, L., Tao, S., Zhang, H., Liu, Y., Yu, Z., Zhao, M., 2011. Distributions and origins of lipid biomarkers in surface sediments from the southern Yellow Sea. *Applied Geochemistry* 26, 1584–1593.
- Xing, L., Jiang, Y., Yuan, Z., Zhang, H., Li, L., Zhou, L., Zhao, M., 2013. Holocene temperature records from the East China Sea mud area southwest of the Cheju Island reconstructed by the U_{37}^k and TEX₈₆ paleothermometers. *Journal of Ocean University of China* 12 (4), 599–604
- Yoon, Y.H., Park, J.S., Soh, H.Y., Hwang, D.J., 2003. Spatial distribution of phytoplankton community and red tide of dinoflagellate, *Prorocentrum donghaiense* in the East China Sea during early summer. *Korean Journal of Environmental Biology* 21, 132–141.
- Zhao, M., Ding, L., Xing, L., Qiao, S., Yang, Z., 2014. Major mid-late Holocene

cooling in the East China Sea revealed by an alkenone sea surface temperature record. *Journal of Ocean University of China* 13:935. doi:10.1007/s11802-014-2641-2.



Appendix

Appendix 1. Data for surface samples during research cruise.

date	Station	Alkenone concentration (ng/L)				U ^{K'} ₃₇	Alkenone temperature (Prahl et al., 1988)	<i>In situ</i> temperature (CTD)
		C _{37:4}	C _{37:3}	C _{37:2}	total C ₃₇			
2007.02	315-13	-	0.1	0.1	0.2	0.6323	17.5	16.7
	315-18	-	-	-	-	-	-	15.2
	315-19	-	-	-	-	-	-	14.8
	315-21	-	-	-	-	-	-	11.3
	316-14	-	-	-	-	-	-	16.6
	316-18	-	-	-	-	-	-	14.1
	316-21	-	-	-	-	-	-	10.2
	317-15	-	-	-	-	-	-	15.8
	317-17	-	-	-	-	-	-	13.6
	317-18	-	-	-	-	-	-	11.8
2007.05	317-16	-	-	-	-	-	-	15.9
2007.08	315-12	-	-	-	-	-	-	29.1
	315-16	-	-	-	-	-	-	28.8
	315-20	-	-	-	-	-	-	28.4
	315-22	-	-	-	-	-	-	26.1
	316-12	-	-	-	-	-	-	29.5
	316-16	-	-	-	-	-	-	28.8
	316-20	-	-	-	-	-	-	28.9
	317-13	-	-	0.1	0.1	-	-	29.7
	317-16	-	-	-	-	-	-	28.5
	317-20	-	-	-	-	-	-	29.7
317-22	-	-	-	-	-	-	29.9	
2007.11	315-12	-	0.1	0.4	0.4	0.8472	23.8	23.0
	315-16	-	-	0.2	0.2	-	-	21.5
	315-20	-	0.1	0.2	0.3	0.5686	15.6	18.2

2007. 11	315-22	-	-	0.1	0.1	-	-	19.9
	316-12	-	-	0.2	0.2	-	-	23.1
	316-16	-	-	0.2	0.2	-	-	22.6
	316-20	-	-	0.1	0.1	-	-	19.3
	316-22	-	0.3	0.6	0.9	0.6786	18.8	20.5
	317-13	-	-	0.2	0.2	-	-	22.8
	317-16	-	-	0.1	0.1	-	-	22.1
	317-20	-	-	-	-	-	-	20.4
	317-22	-	0.1	0.2	0.3	0.6919	19.2	21.0
2008. 02	315-12	-	0.2	0.2	0.5	0.5603	15.3	17.4
	315-16	-	-	-	-	-	-	14.8
	315-20	-	-	-	-	-	-	11.6
	315-22	-	-	-	-	-	-	8.0
	316-12	-	0.2	0.3	0.6	0.6070	16.7	17.4
	316-16	-	-	-	-	-	-	14.8
	316-20	-	-	-	-	-	-	10.0
	316-22	-	-	-	-	-	-	8.4
	317-13	-	0.1	0.1	0.2	0.6108	16.8	16.3
	317-16	-	-	-	-	-	-	12.8
	317-20	-	-	-	-	-	-	9.9
	317-22	-	-	-	-	-	-	9.4
2008. 05	315-12	-	3.0	7.6	10.6	0.7191	17.6	20.2
	315-16	-	-	-	-	0.6373	17.4	18.6
	315-20	-	0.0	0.1	0.1	0.6321	19.1	15.4
	315-22	-	0.1	0.1	0.2	0.6870	19.2	17.6
	316-12	-	0.7	1.3	2.0	0.6457	17.8	19.1
	316-16	-	0.4	0.4	0.8	0.5425	14.8	16.7
	316-20	-	-	-	-	-	-	14.7
	316-22	-	0.0	0.1	0.1	0.5051	13.7	15.0
	317-13	-	0.5	0.9	1.4	0.6266	17.3	18.1
	317-17	-	0.1	0.2	0.3	0.6615	18.3	15.4
	317-20	-	0.2	0.2	0.3	0.4569	12.3	15.2

2008. 05	317-22	-	0.3	0.2	0.5	0.4575	12.3	15.6
2008. 08	315-22	-	-	-	-	-	-	27.7
2009. 02	315-12	-	0.2	0.2	0.4	0.5747	15.7	17.5
	315-14	-	-	-	-	-	-	16.9
	315-16	-	-	-	-	-	-	15.8
	315-18	-	-	-	-	-	-	15.2
	315-20	-	-	-	-	-	-	12.0
	315-22	-	-	-	-	-	-	9.1
	316-13	-	0.2	0.3	0.5	0.5283	14.4	17.7
	316-15	-	-	-	-	-	-	16.5
	316-17	-	0.1	0.1	0.1	0.4500	12.1	14.2
	316-18	-	-	-	-	-	-	13.1
	316-21	-	-	-	-	-	-	9.6
	317-13	-	0.2	0.2	0.4	0.5181	14.1	17.2
	317-15	-	-	-	-	-	-	14.8
	317-18	-	-	-	-	-	-	12.2
	317-20	-	-	-	-	-	-	10.7
	317-22	-	-	-	-	-	-	10.5
2009. 05	315-12	-	0.4	0.7	1.1	0.6545	18.1	19.4
	315-13	-	0.1	0.3	0.4	0.6458	17.8	19.1
	315-15	-	0.1	0.1	0.2	0.6068	16.7	18.3
	315-17	-	-	-	-	-	-	17.2
	315-19	-	-	-	-	-	-	16.4
	315-21	-	-	-	-	-	-	14.8
	316-12	-	0.4	1.1	1.5	0.7166	19.9	20.2
	316-14	-	0.1	0.2	0.3	0.6180	17.0	18.6
	316-16	-	-	-	-	-	-	18.3
	316-18	-	-	-	-	-	-	16.3
	316-20	-	-	-	-	-	-	14.9
	316-22	-	-	-	-	-	-	15.1
	317-13	-	0.2	0.4	0.5	0.6953	19.3	18.5
	317-15	-	-	-	-	-	-	18.1

2009. 05	317-17	-	-	-	-	-	-	16.7
2009. 11	315-15	-	0.1	0.3	0.5	0.7549	21.1	21.2
	315-20	-	0.1	0.2	0.3	0.717	19.9	19.8
	316-15	-	0.1	0.3	0.3	0.7958	22.3	21.4
	316-17	-	0.0	0.1	0.1	0.7687	21.5	20.8
	316-22	-	-	-	-	-	-	19.3
	317-13	-	0.1	0.3	0.3	0.8191	22.9	22.1
	317-16	-	-	0.1	0.1	-	-	21.0
2010. 08	315-13	-	-	0.5	0.5	-	-	28.9
	315-17	-	-	0.3	0.3	-	-	29.8
	315-20	-	-	-	-	-	-	29.0
	315-22	-	-	-	-	-	-	28.1
	316-12	-	-	0.9	0.9	-	-	29.5
	316-16	-	-	-	-	-	-	29.1
	316-19	-	-	1.7	1.7	-	-	29.3
	316-21	-	-	0.1	0.1	-	-	28.2
	317-14	-	-	2.4	2.4	-	-	29.1
	317-17	-	-	1.2	1.2	-	-	29.6
	317-19	-	-	2.6	2.6	-	-	29.3

Appendix 2. Data for subsurface samples during research cruise.

date	Station		Alkenone concentration (ng/L)				U ^K ₃₇	Alkenone temperature (Prah et al., 1988)	<i>In situ</i> temperature (CTD)
			C _{37:4}	C _{37:3}	C _{37:2}	total C ₃₇			
2007.11	317-13	20 m	-	-	0.3	0.3	-	-	22.8
		50 m	-	0.0	0.3	0.4	0.9050	25.5	22.8
	315-22	20 m	-	0.1	0.2	0.3	0.7011	19.5	20.0
		30 m	-	0.0	0.1	0.1	0.7181	20.0	20.0
2008.02	315-12	20 m	-	0.2	0.3	5.0	0.5520	15.1	17.2
		50 m	-	0.2	0.2	0.4	0.5655	15.5	17.3
	317-13	20 m	-	0.1	0.1	0.2	0.5887	16.2	16.4
		50 m	-	0.1	0.1	0.2	0.5969	16.4	16.7
2008.05	315-12	20 m	-	4.1	8.9	13.1	0.6835	19.0	19.6
		50 m	-	0.4	0.9	1.3	0.6650	18.4	18.1
	317-13	20 m	-	0.5	0.6	1.1	0.5697	15.6	18.1
		50 m	-	0.1	0.1	0.2	0.5246	14.3	14.7
2008.08	315-12	20 m	-	-	-	-	-	-	28.6
		50 m	-	0.2	0.4	0.5	0.6715	18.6	16.7
	317-13	20 m	-	-	0.2	0.2	-	-	24.8
		50 m	-	-	0.1	0.1	-	-	13.9
2009.02	315-12	20 m	-	0.3	0.3	0.5	0.5334	14.5	17.5
		50 m	-	-	-	-	-	-	17.2
	317-13	20 m	-	-	-	-	-	-	17.2
		50 m	-	-	-	-	-	-	16.8
2009.05	315-12	20 m	-	0.4	0.7	1.0	0.6473	17.9	19.2
		50 m	-	0.2	0.3	0.5	0.5793	15.9	17.4
	317-13	20 m	-	0.5	0.8	1.3	0.6047	16.6	16.7
		50 m	-	0.1	0.1	0.2	0.5651	15.5	15.8
2009.08	315-12	20 m	-	-	0.2	0.2	-	-	29.1
		50 m	-	0.1	0.3	0.4	0.6905	19.2	18.7
	317-13	20 m	-	0.2	1.4	1.6	0.8705	24.5	21.3
		50 m	-	-	0.3	0.3	-	-	18.8

2009. 11	315 -12	20 m	-	0.3	0.5	0.8	0.6691	18.5	21.2
		50 m	-	0.1	0.4	0.5	0.7647	21.3	21.2
	317 -13	20 m	-	0.1	0.4	0.5	0.8320	23.3	22.1
		50 m	-	0.1	0.3	0.4	0.8337	23.4	22.1
2010. 08	315 -12	20 m	-	-	1.3	1.3	-	-	25.8
		50 m	-	-	0.1	0.1	-	-	18.6
	317 -13	20 m	-	-	0.6	0.6	-	-	26.3
		50 m	-	-	0.4	0.4	-	-	19.2

